LBL-13704
Preprint

Lawrence Berkeley Laboratory

UNIVERSITY OF CALIFORNIA

RECEIVED
LAWRENCE
BERKELEY LABORATORY

FEB 10 1982

LIBRARY AND
DOCUMENTS SECTION

Materials & Molecular Research Division

Submitted to the Journal of Materials Science

DEFECTS IN ANTIFERROMAGNETIC NICKEL OXIDE

D.J. Coates, J.W. Evans and K.H. Westmacott

December 1981

TWO-WEEK LOAN COPY

This is a Library Circulating Copy which may be borrowed for two weeks. For a personal retention copy, call Tech. Info. Division, Ext. 6782

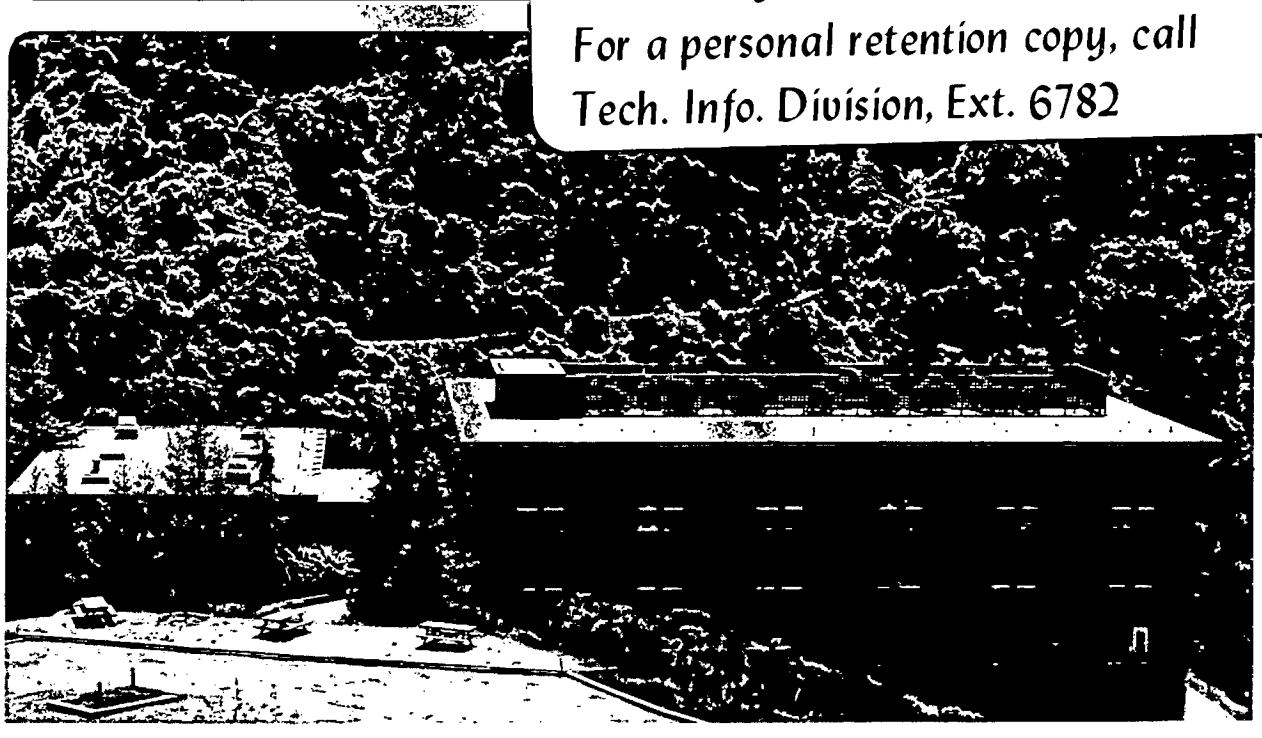

LBL-13704 c.2

Prepared for the U.S. Department of Energy under Contract W-7405-ENG-48

DISCLAIMER

This document was prepared as an account of work sponsored by the United States Government. While this document is believed to contain correct information, neither the United States Government nor any agency thereof, nor the Regents of the University of California, nor any of their employees, makes any warranty, express or implied, or assumes any legal responsibility for the accuracy, completeness, or usefulness of any information, apparatus, product, or process disclosed, or represents that its use would not infringe privately owned rights. Reference herein to any specific commercial product, process, or service by its trade name, trademark, manufacturer, or otherwise, does not necessarily constitute or imply its endorsement, recommendation, or favoring by the United States Government or any agency thereof, or the Regents of the University of California. The views and opinions of authors expressed herein do not necessarily state or reflect those of the United States Government or any agency thereof or the Regents of the University of California.

DEFECTS IN ANTIFERROMAGNETIC NICKEL OXIDE

D.J. Coates, J.W. Evans and K.H. Westmacott
Materials and Molecular Research Division
Lawrence Berkeley Laboratory

and

Materials Science and Mineral Engineering
University of California
Berkeley, California 94720

This work was supported by the Division of Materials Sciences, Office of Basic Energy Sciences, U.S. Department of Energy under Contract No. W-7405-ENG-48.

INTRODUCTION

The reduction of nickel oxide to metallic nickel by means of gaseous reductants, particularly hydrogen, has been the subject of numerous investigations (1-6). The techniques employed usually involve measuring macroscopic properties of the system, e.g. weight change, during the reduction experiment and then manipulating the data to produce a mathematical formulation of a general rate equation for the system (e.g. Szekeley and Evans (7,8)). Whilst this type of investigation can be very successful anomalies sometimes arise due to the fact that reduction processes occur on an atomic scale and possibly may be influenced by the presence of microscopic features such as grain boundaries or dislocations in the nickel oxide. In many reducing reactions there is a considerable induction period when no reaction, as measured macroscopically, occurs. This induction period is associated with the formation of nuclei of the reduced species which form only after the oxide has become sufficiently supersaturated with respect to the metal as oxygen is removed by the reducing gas. Nucleation of the reduction reaction occurs only at energetically favourable sites, so that the number of nuclei formed per unit surface area depends significantly on the condition of the surface.

Previous investigations have shown that the induction period for nickel oxide reduction is shortened by a factor of three to four and the rate of reaction is increased by a factor of two to three at 300-350°C when subjected to prior irradiation with 260 MeV protons (9). An increased reduction rate has also been observed with mechanically worked nickel oxide (10). In both cases the effects were attributed to the crystal distortion produced by the radiation or plastic deformation

processes resulting in higher energy sites in the crystal surface which facilitate the formation of nickel nuclei. Further evidence of the influence of the microstructure of the nickel oxide on its reduction behaviour is the well-documented observance of a change in activation energy of the reduction reaction at the Neél transformation temperature, T_N(∿250°C). Above this temperature nickel oxide is cubic and has the NaCl structure. Below this temperature NiO is antiferromagnetic and the magnetic spins of the nickel ions lying in adjacent (111) planes are oriented anti-parallel to one another. As a result of magnetostrictive interactions the lattice contracts slightly along a <111> direction giving a rhombohedral structure. Different regions, or domains, in a given grain may contract along different <111> directions. The boundaries between such domains are low-angle twin boundaries and lie along {110} and {111} planes. These domain walls have been observed in nickel oxide using neutron diffraction (11,12), specular reflection (13) and electron microscopy (14-16), although only those domain boundaries lying on {110} planes have previously been imaged by electron microscopy. In order to observe the domains in transmission electron microscopy, two-beam dynamical conditions have to be used. From the resulting images certain features of the domains, such as direction of slope of the boundaries and contraction direction of the lattice can be deduced (15). The observation that the density of nuclei also changes at the transformation temperature (5) suggests that the domain boundaries that intersect the surface of the specimens at temperatures below T_N may affect the distribution of energetically favourable nucleation sites.

The present work reports some features of the domain boundaries in

nickel oxide, as well as some other crystal defects, as observed by transmission electron microscopy. Preliminary results of in-situ reduction experiments on nickel oxide are also reported.

EXPERIMENTAL

Specimens were obtained from single crystal boules of nickel oxide by machining, abrading and ion-beam thinning to electron transparency. Further details of the specimens and preparation technique have been reported previously (17). Specimens were examined on a 650 keV Hitachi microscope with double-tilt and heating stages. In-situ reduction experiments were carried out in a Gatan environmental cell with a single-tilt platinum ribbon heating stage.

RESULTS

Previously only one set of domain boundaries have been imaged in electron microscopy, due to the limitations of the crystallographic orientations of the specimens used (the foils had (100) orientations so that {100} type domain walls were not able to give fringe contrast). In the present work thin foils of nickel oxide were prepared with their surfaces approximately parallel to (111), (110) as well as (100) zone axes. Figure 1 shows a number of somain boundaries imaged under two beam conditions in a (111) oriented foil. The domain boundaries intersect at various angles and hence must be both {100} and {110} type boundaries. In some areas there appears to be some interaction between dislocations in the matrix and the domain boundaries, this is illustrated more graphically below. It is also apparent that the slightly different orientations of the lattice in adjacent domains gives rise to different contrast conditions so

that the matrix appears alternatively lighter or darker. The orientations of the domain boundaries can be analyzed by trace analysis. Figure 2 shows the results of such an analysis on two domain boundaries imaged under two-beam conditions ($\underline{g}$ = 220). Figure 2a is a bright-field micrograph and Figure 2b a dark-field micrograph of the same area. The boundary labelled X is a (110) type boundary, and that labelled Y is a (100) type boundary.

The fringe patterns of the boundaries are due to dynamical coupling of the two-beams, which has been dealt with theoretically by Gevers et al. (15). The nature of the edge fringes in each boundary under bright field conditions is different, i.e. one is bright and one dark. Under dark-field imaging conditions the nature of the edge fringes in both domain boundaries is similar, both being bright in one boundary and dark in the other. According to the theoretical treatment and observations of Gevers et al. (15), the fringe corresponding to the intersection of the boundary with the upper surface is similar in nature in bright-field and dark-field images, whereas the lower edge fringe is 'pseudo-complementary'. The bottom and top edges of the domain boundaries in Figure 2 are labelled 'B' and 'T' respectively. The boundaries thus both slope in the same direction.

Domain boundaries were observed to move readily through the foil due to the thermal stresses associated with the beam heating of the specimen. This is illustrated by the movement of the domain boundaries between the exposures of figures 2a and 2b with respect to the arrowed dislocation. Movement of the boundaries could be prevented by spreading the electron

beam to dissipate the heating effect. Movement of the boundaries was also restricted by dislocation pinning. Figures 3 and 4 show the effects of dislocations on the domain boundary configuration. In some cases the pinned configuration was very stable and no amount of beam convergence induced movement of the domain boundaries. In an associated series of experiments, specimens were heated in-situ and then cooled through the Neél temperature. In some areas domain boundaries were observed to reappear in approximately the same positions they were in before the heating cycle. These boundaries were generally the ones pinned by dislocations. Similar observations have been reported in antiferromagnetic MnO where dislocations generated by the formation of Mn_3O_4 precipitates, as well as the precipitates themselves, were found to pin the domain boundaries (18).

Stable configurations of domain boundaries were also observed associated with low-angle grain boundaries within the nominally single crystal material. Figure 5 shows such a configuration, the planar defects toward the top of the micrograph (labelled A) are low angle grain boundaries, those toward the bottom (labelled B) are domain boundaries. Very little movement of these domain boundaries was found, even after extended periods of electron beam impingement.

Fringe patterns were observed associated with some individual dislocations, as well as with the extended domain boundaries. The dislocation above the intersection of the domain boundaries in Figure 2a shows such a feature. These were usually broader in extent at one end of the dislocation and grew thinner, sometimes disappearing, toward the centre of the dislocation. Figure 6 shows a stereo pair of some dislocations with associated fringe patterns from which it is seen that the patterns are clearly associated with

the dislocations. The fringe patterns disappeared when the specimens were heated above the Néel temperature, indicating that they are antiferromagnetic domain boundaries, so that it is apparent that some dislocations can stabilize small domains associated with them.

Another feature of the nickel oxide structure which is apparent in a number of micrographs is the presence of dislocation loops (see Figures 5 and 6). Contrast experiments were conducted to determine the nature of the loops (see 19), an example of which is shown in Figure 7. In Figure 7a the deviation parameter, s, has a positive value, as shown by the diffraction pattern, and the loop contrast lies outside the actual position of the loop. In Figure 7b s is negative and the loop contrast lies inside the loop position. From these observations, and the change in shape of the loop with further tilting, it is deduced that the loops are due to clusters of vacancies in the NiO lattice and are similar to those found in MgO (20,21).

In-situ reduction experiments have been carried out and some preliminary results are shown in Figures 8 and 9. A nickel oxide specimen was heated in the environmental cell. The reducing temperature was about 220-250°C. A $10H_2$:90He gas mixture was used as the reductant at a pressure of 100 Torr. Figure 8 shows an area after 13 min and 31 min exposure and Figure 9 shows the same area after 41 min and 49 min exposure. Initially small nuclei of nickel developed and gradually covered the surface of the nickel oxide. After 13 min exposure (Figure 8a) much of the NiO in the micrograph is covered with small nickel grains, with some areas apparently unaffected. With further reduction these areas also became covered with nickel grains. At a later stage many of the small nickel nuclei appeared unchanged, but in some areas 'colonies' of nickel developed. Some of these colonies are arrowed in Figure 8b and are aligned along a discrete band on the surface of the NiO, suggesting there may be some linear microstructural

feature in the NiO influencing the formation of the colonies. After 41 min exposure (Figure 9a) no change in the small nickel nuclei is observed, but the colonies have grown in size. Figure 9b shows the area after 49 min exposure after which the specimen was cooled to room temperature. The specimen has been tilted to image any domain boundaries in the NiO substrate. Although the limitations of a single-tilt stage means it is difficult to obtain precise two-beam conditions in order to obtain good contrast conditions, some images of domain boundaries were obtained. One such boundary lies near the top of Figure 9b, parallel to the row of colonies arrowed in Figure 8b. Another domain boundary lies along the line of these colonies and may thus have influenced the formation of the colonies.

DISCUSSION AND CONCLUSIONS

The micrographs show clearly the presence of both {100} and {110} type domain boundaries which were not imaged in previous t.e.m. work (16). It was found that thermal stresses can cause a redistribution of the domain walls although some configurations were stabilized by dislocation pinning. This could have a significant effect on the reduction of the nickel oxide at temperatures below T_N if, in fact, the nucleation process is influenced by the domain boundaries. Thus an increased number of dislocations in the original nickel oxide resulting from prior working will cause pinning and retention of domain boundaries which might otherwise migrate to grain boundaries and be eliminated. Also individual dislocations may have small domains associated with them. Thus previously worked nickel oxide will have a greater density of domain boundaries at reducing temperatures (below T_N) than will fully annealed specimens.

Previous observations (17) indicate that dislocations themselves may have little influence on the nucleation sites of nickel on nickel oxide. The increased density of domain boundaries may provide an alternative explanation for the increase in reduction rates observed in mechanically worked specimens and presumed to be due to an increased density of nucleation sites.

Preliminary investigations into the reduction of nickel oxide indicate that domain boundaries may well influence the distribution of nickel "colonies' which are apparently a result of accelerated reduction of the nickel oxide in discrete regions. However, the evidence so far is not unequivocal. Further experiments are proceeding using an improved design furnace in the environmental cell, by which it is hoped to obtain unambiguous information concerning the role of domain boundaries in the nucleation of nickel.

The presence of vacancy loops in annealed nickel oxide, similar to those found in MgO (20,21) has been established. In MgO the loops appeared in rows and were attributed to have originated as elongated dislocation dipoles. Rows of dislocation loops have also been observed in the wake of dislocations in NiO(16) suggesting a similar mode of formation, although in the present study the loops appear individually dispersed and not associated with dislocations.

This work was supported by the Division of Materials Sciences, Office of Basic Energy Sciences, U.S. Department of Energy under contract no. W-7405-Eng-48.

REFERENCES

1. PARRAVANO, G.; J. Am. Chem. Soc. 74, 1194 (1952).
2. SZEKELEY, J., LIN, C.I., and SOHN, H.Y., Chem. Eng. Sci. 28, 1975 (1973).
3. EVANS, J.W., Ph.D. Dissertation, State University of New York at Buffalo, 1970.
4. CHIESA, F. and RIGAUD, M., Can. J. Chem. Eng. 49, 617 (1971).
5. ROMAN, A. and DELMON, B., Compt. Rend. Ser. B. 269, 801 (1969).
6. ROMAN, A. and DELMON, B. Compt. Rend. Ser. B. 271, 77 (1970).
7. SZEKELEY, J. and EVANS, J.W., Met. Trans. 2, 1691 (1971).
8. SZEKELEY, J. and EVANS, J.W., Met. Trans. 2, 1699 (1971).
9. SIMNAD, M.T., SMOLUCHOWSKI, R. and SPILNERS, A., J. Appl. Phys. 29, 1930 (1958).
10. IIDA, Y. and SHIMADA, K., Bull. Chem. Soc. Jap. 33, 1194 (1964).
11. MARMEGGI, J.C. and BARUCHEL, J., J. Mag. and Mag. Mats. 10, 14 (1979).
12. ROTH, W.L., J. Appl. Phys. 31, 2000 (1960).
13. SLACK, G.A., J. Appl. Phys. 31, 1571 (1960).
14. DELAVIGNETTE, P. and AMELINCKX, S., App. Phys. Lett. 2, 236 (1963).
15. GEVERS, R., DELAVIGNETTE, P., BLANK, H. and AMELINCKX, S., Phys. Stat. Sol. 4, 383 (1964).
16. GEVERS, R., DELAVIGNETTE, P., BLANK, H., van LANDUYT, J. and AMELINCKX, S., Phys. Stat. Sol. 5, 595 (1964).
17. LITTLE, J., EVANS, J.W., and WESTMACOTT, K., Met. Trans. 11B, 519 (1980).
18. BARBER, D.J. and EVANS, R.G., J. Mat. Sci. 6, 1237 (1971).
19. THOMAS, G. and GORINGE, M.J., Transmission Electron Microscopy, Wiley, New York, 1979.
20. GROVES, G.W. and KELLY, A., Phil. Mag. 6, 1527 (1961).
21. GROVES, G.W. and KELLY A., Phil. Mag. 7, 892 (1962).

FIGURE CAPTIONS

Figure 1 Antiferromagnetic domain boundaries in nickel oxide

Figure 2 Bright-field and dark-field of domain boundaries, x-(110) type boundary, Y-(100) type boundary, B-bottom edge, T-top edge.

Figure 3 Interaction of domain boundaries with dislocations

Figure 4 Interaction of two domain boundaries with two dislocations, forming a small domain

Figure 5 Bright-field micrograph of low angle grain boundaries (A) and domain boundaries (B)

Figure 6 Stereographic pair (tilt$\sim$10°) of dislocations and associated domain boundaries

Figure 7 Dislocation loop in NiO, with $\underline{s} > 0$ and $\underline{s} < 0$

Figure 8 In-situ reduction of NiO in $10H_2$:90He after 13 and 31 min reduction (T $\sim$ 220-250°C)

Figure 9 In-situ reduction of NiO in $10H_2$:90He after 41 and 49 min reduction (T $\sim$ 200-250°C).

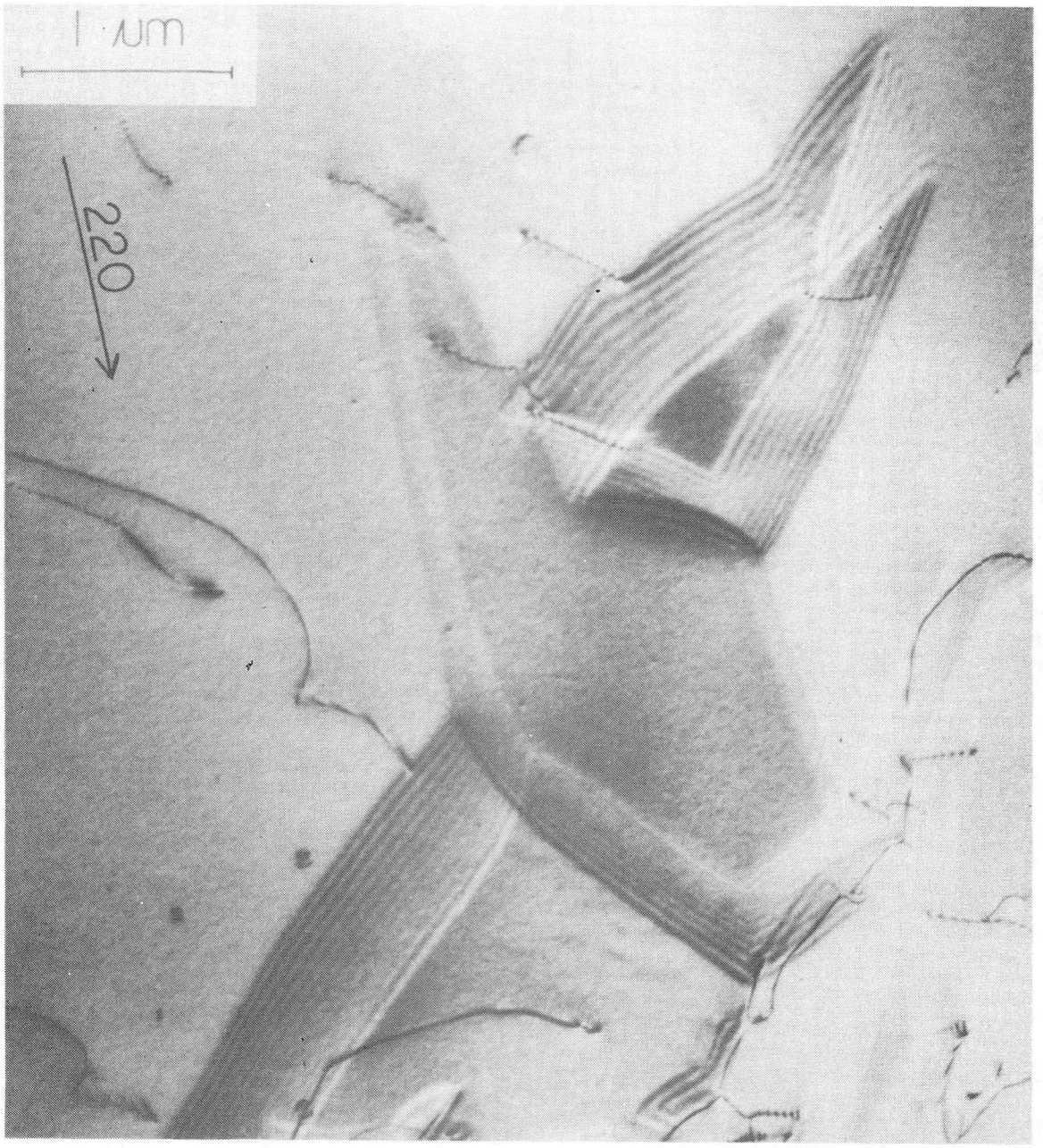

Figure 1. Antiferromagnetic domain boundaries in nickel oxide.

XBB 810-11372

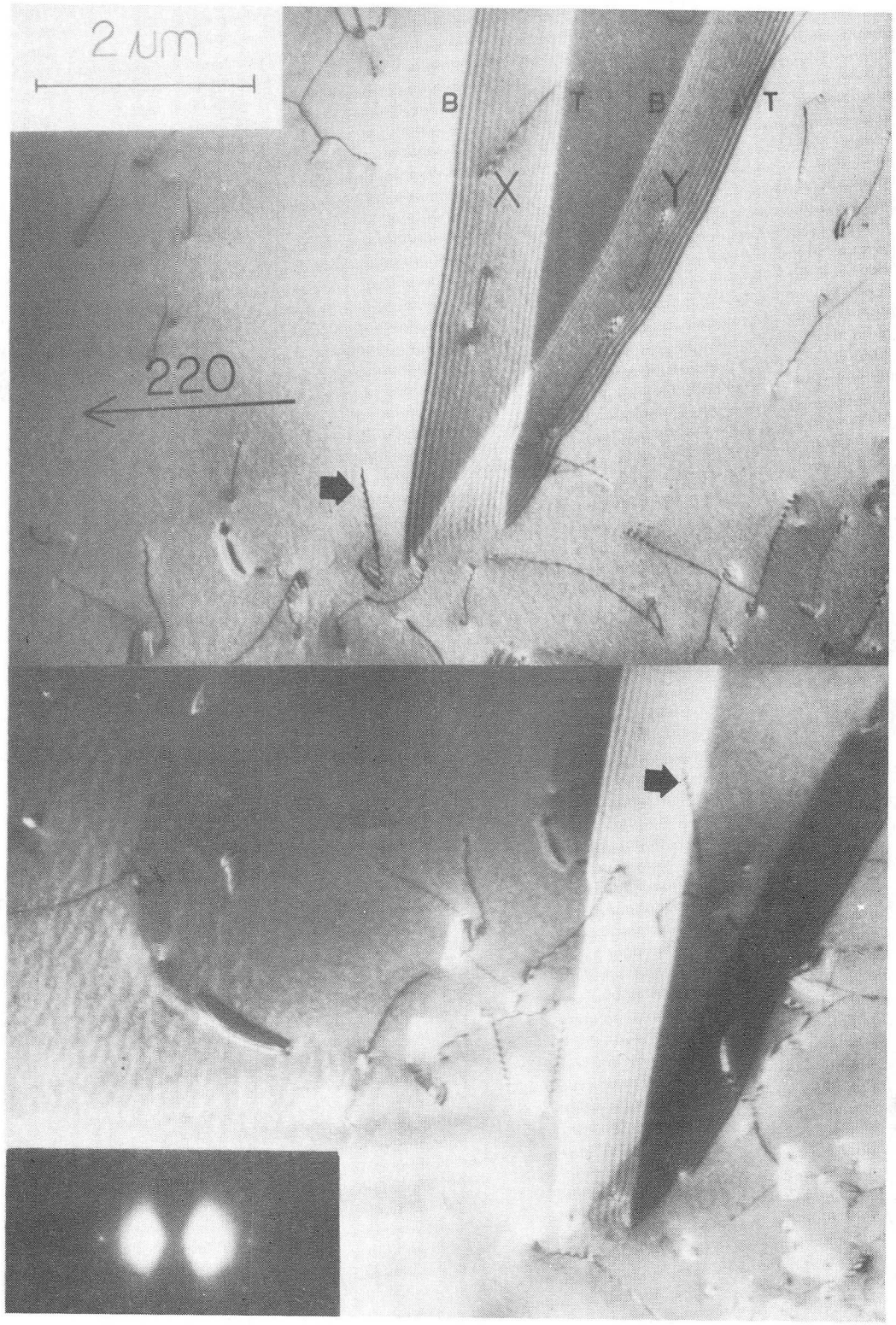

Figure 2. Bright-field and dark-field of domain boundaries, x-(110) type boundary, Y-(100) type boundary, B-bottom edge, T-top edge. XBB 810-11373

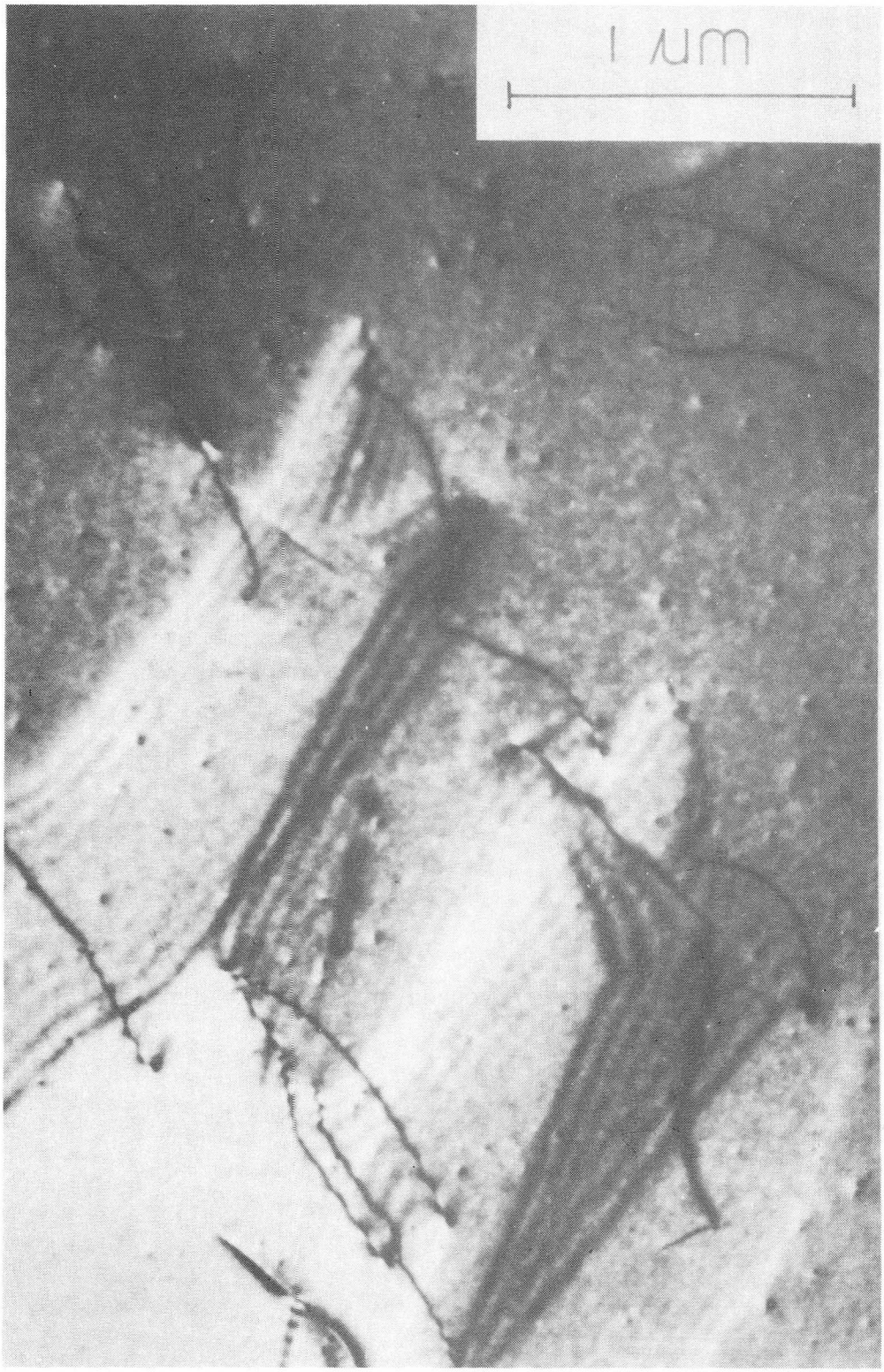

Figure 3. Interaction of domain boundaries with dislocations. XBB 810-9914

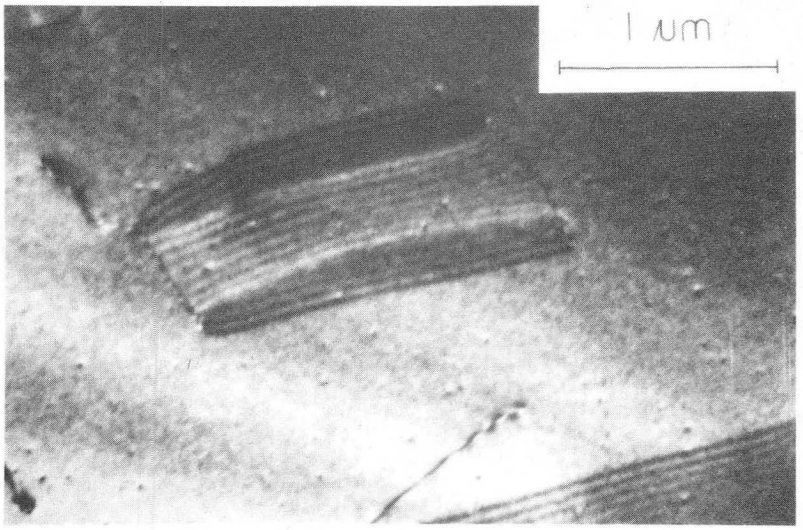

XBB 810-9915

Figure 4 Interaction of two domain boundaries with two dislocations, forming a small domain

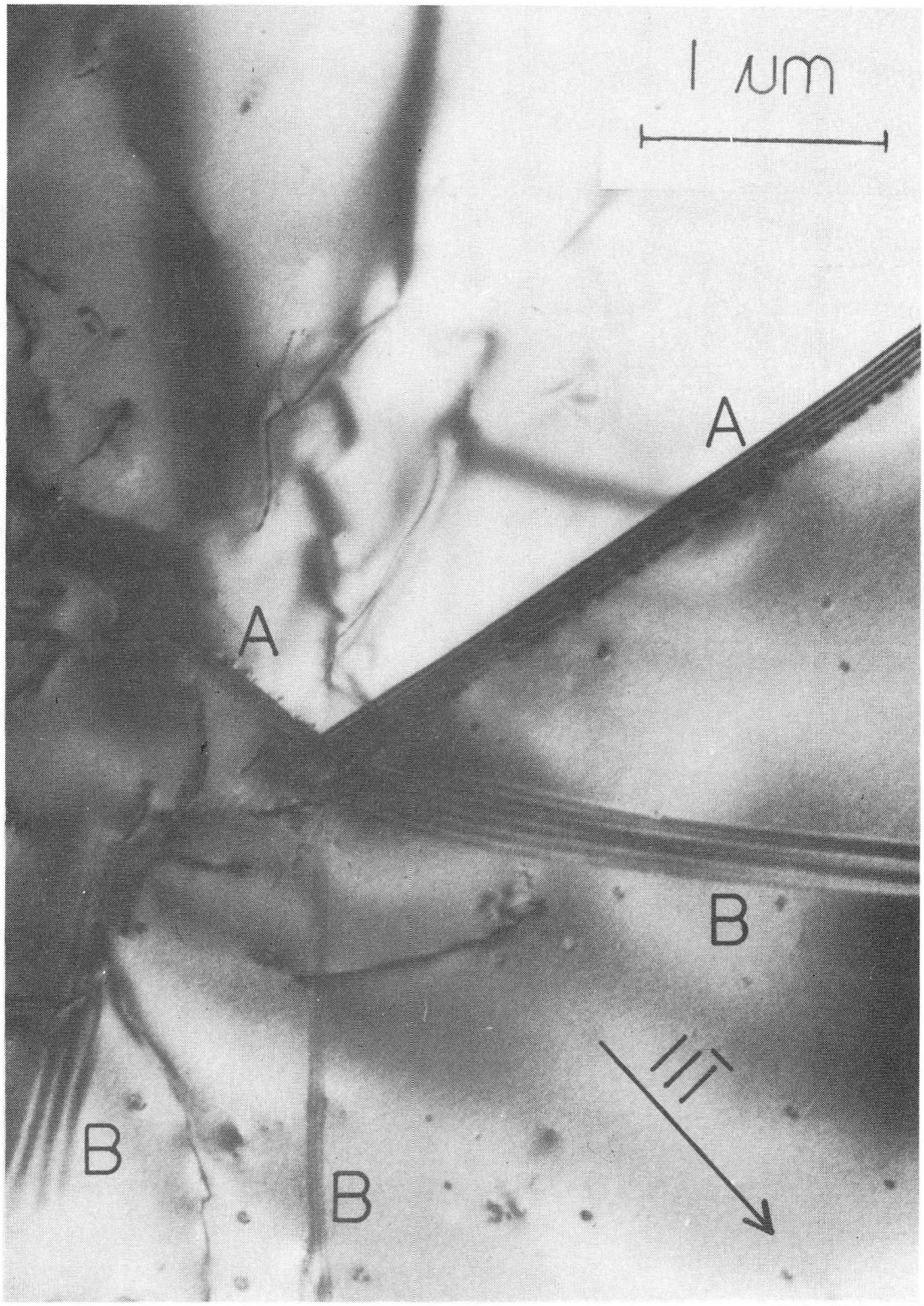

Figure 5. Bright-field micrograph of low angle grain boundaries (A) and domain boundaries (B). XBB 810-11371

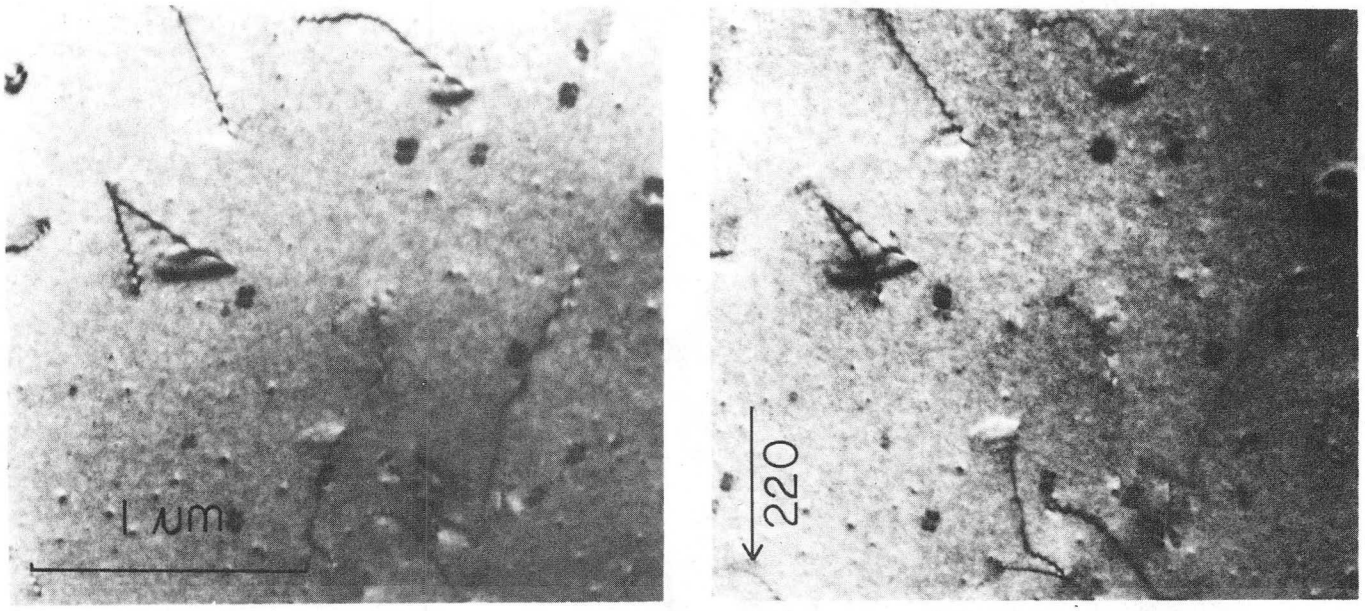

XBB 8111-11376

Figure 6 Stereographic pair (tilt∿10°) of dislocations and associated domain boundaries

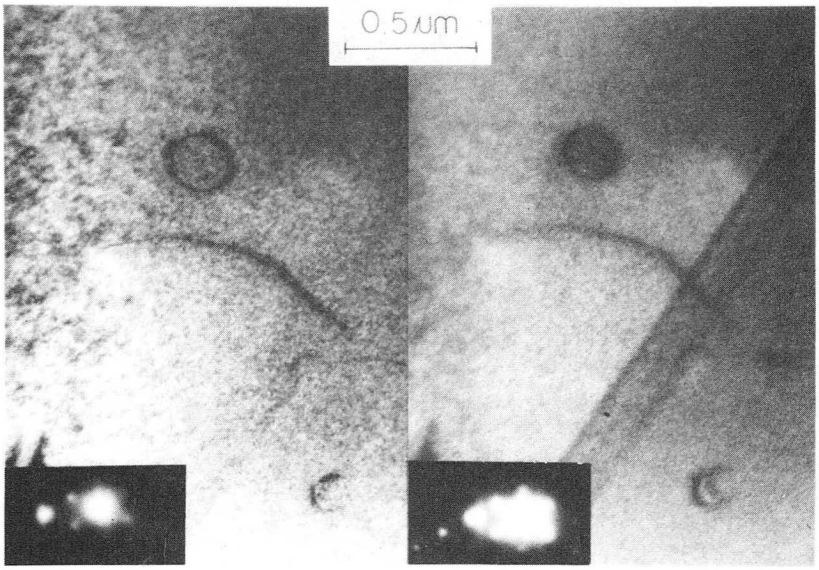

XBB 810-9921

Figure 7 Dislocation loop in NiO, with $\underline{s} > 0$ and $\underline{s} < 0$

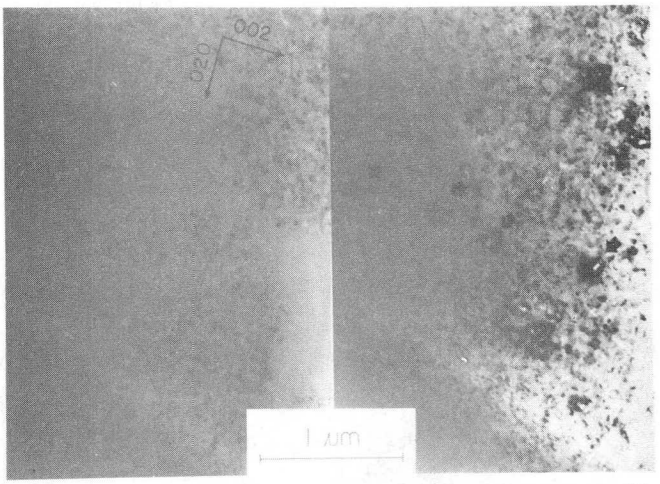

XBB 8111-11374

Figure 8 In-situ reduction of NiO in $10H_2$:90He after 13 and 31 min reduction (T ∿ 220-250°C)

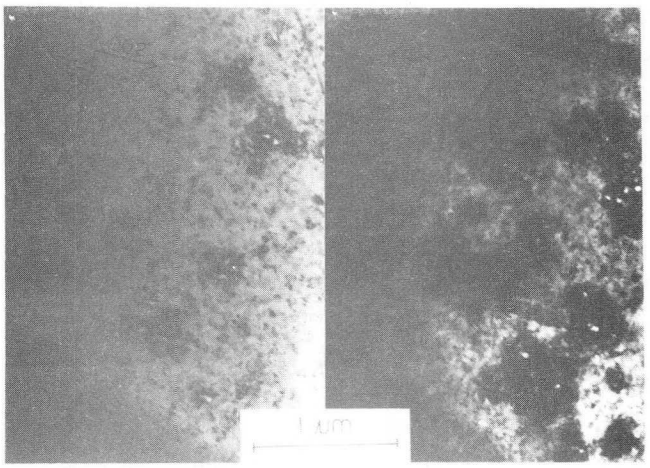

XBB 8111-11375

Figure 9 In-situ reduction of NiO in $10H_2$:90He after 41 and 49 min reduction (T ∿ 200-250°C).

This report was done with support from the Department of Energy. Any conclusions or opinions expressed in this report represent solely those of the author(s) and not necessarily those of The Regents of the University of California, the Lawrence Berkeley Laboratory or the Department of Energy.

Reference to a company or product name does not imply approval or recommendation of the product by the University of California or the U.S. Department of Energy to the exclusion of others that may be suitable.

TECHNICAL INFORMATION DEPARTMENT
LAWRENCE BERKELEY LABORATORY
UNIVERSITY OF CALIFORNIA
BERKELEY, CALIFORNIA 94720